

See discussions, stats, and author profiles for this publication at: <https://www.researchgate.net/publication/223135427>

# High-Throughput Analysis of Protein-Protein Interactions in Picoliter-Volume Droplets Using Fluorescence Polarization

ARTICLE in ANALYTICAL CHEMISTRY · APRIL 2012

Impact Factor: 5.64 · DOI: 10.1021/ac300414g · Source: PubMed

---

CITATIONS

37

---

READS

34

5 AUTHORS, INCLUDING:



**Dong-Ku Kang**

University of California, Irvine

34 PUBLICATIONS 630 CITATIONS

SEE PROFILE



**Hyun Park**

Chungbuk National University

7 PUBLICATIONS 82 CITATIONS

SEE PROFILE



**Soo-Ik Chang**

Chungbuk National University

91 PUBLICATIONS 1,650 CITATIONS

SEE PROFILE

# High-Throughput Analysis of Protein–Protein Interactions in Picoliter-Volume Droplets Using Fluorescence Polarization

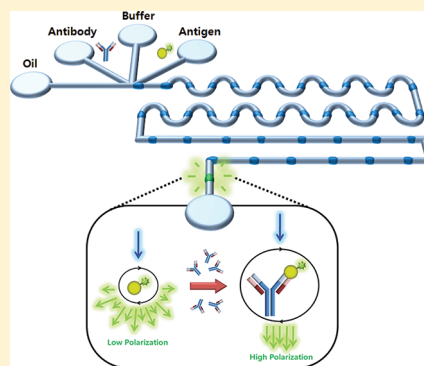
Jae-Won Choi,<sup>†</sup> Dong-Ku Kang,<sup>†,‡</sup> Hyun Park,<sup>†</sup> Andrew J. deMello,<sup>§</sup> and Soo-Ik Chang<sup>\*,†</sup>

<sup>†</sup>Department of Biochemistry, Chungbuk National University, Cheongju 361-763, Republic of Korea,

<sup>‡</sup>Department of Chemistry, Imperial College London, London SW7 2AZ, United Kingdom,

<sup>§</sup>Department of Chemistry and Applied Biosciences, ETH Zürich, Zürich CH-8093, Switzerland

**ABSTRACT:** Droplet-based microfluidic systems have emerged as a powerful platform for performing high-throughput biological experimentation. In addition, fluorescence polarization has been shown to be effective in reporting a diversity of bimolecular events such as protein–protein, DNA–protein, DNA–DNA, receptor–ligand, enzyme–substrate, and protein–drug interactions. Herein, we report the use of fluorescence polarization for high-throughput protein–protein interaction analysis in a droplet-based microfluidic system. To demonstrate the efficacy of the approach, we investigate the interaction between angiogenin (ANG) and antiangiogenin antibody (anti-ANG Ab) and demonstrate the efficient extraction of dissociation constants ( $K_D = 10.4 \pm 3.3$  nM) within short time periods.



In recent years, droplet-based (or segmented-flow) microfluidic systems have emerged as a powerful technological platform for performing high-throughput chemical and biological experimentation.<sup>1,2</sup> Droplet-based systems are especially well suited for this purpose since they overcome many of the problematic issues that impact continuous-flow formats, such as sample dilution due to Taylor dispersion, solute surface interactions, cross-contamination when performing multiple experiments, and the need for excessive reagent volumes. Moreover, the manipulation of picoliter-volume droplets (surrounded by an immiscible continuous phase) through winding channels is beneficial in enabling rapid and efficient mixing of the contained reagents. Since droplets may be generated at kilohertz frequencies, enormous experimental data sets can also be amassed in short times allowing complex statistical analyses of multicomponent systems.<sup>3–5</sup>

While droplet-based microfluidic systems are efficient in generating vast amounts of chemical and biological information, the development of sensitive detection methods is critical in allowing this information to be extracted and utilized. To this end, a variety of optical detection methods for probing segmented flows in real time have been developed. These include methods based on time-integrated fluorescence spectroscopy,<sup>6,7</sup> fluorescence lifetime imaging (FLIM),<sup>8,9</sup> fluorescence resonance energy transfer (FRET),<sup>10–14</sup> FT-IR imaging,<sup>15</sup> mass spectrometry,<sup>16</sup> and surface enhanced Raman scattering (SERS).<sup>17,18</sup> Detection based on FRET has been especially useful in probing biomolecular interactions. Indeed, we previously described the use of FRET for high-throughput analysis of protein–protein interactions in picoliter-volume droplets.<sup>14</sup> Unfortunately, when screening therapeutic antibodies against an antigen, FRET employs both

a donor and acceptor dye. This means that multiple labeling chemistries are required for each antibody.

Fluorescence polarization (FP), on the other hand, is a homogeneous technique that does not require the separation of bound and free species from the analytical sample to allow analysis. Methods that depend on separation are not only time-consuming but also disturb reaction equilibria and therefore prevent accurate quantification of binding.<sup>19</sup> FP measurements are based on the principle of photoselective excitation of a population of fluorophores using polarized radiation. In simple terms, fluorophores with dipoles parallel to the excitation radiation will absorb photons, whereas those with dipoles perpendicular to excitation radiation will not. This leads to partially polarized fluorescence emission. In free solution, the observed emission will be depolarized via rotational diffusion. This rotational diffusion (and thus depolarization) can be significantly hindered if the fluorophore binds to a larger molecule or exists in a high-viscosity medium.

Accordingly, FP measurements have been used to probe many biological reactions such as receptor–ligand binding,<sup>20</sup> DNA hybridization,<sup>21</sup> DNA–protein binding,<sup>22,23</sup> peptide–protein binding,<sup>24</sup> immunoassays,<sup>25,26</sup> and enzymatic degradation.<sup>27–29</sup> In addition, recent important advances of FP showing the measurement of the DNA wrapping and close contact involved in protein–DNA binding and application in immunoassays have been reported.<sup>30,31</sup> FP detection is particularly advantageous since it is truly a homogeneous assay format, allows for real-time (kinetic) measurements, and is

**Received:** February 12, 2012

**Accepted:** March 25, 2012

**Published:** March 25, 2012



insensitive to concentration variations. For these reasons, we report herein the use of FP detection in a droplet-based microfluidic system. Specifically, we investigate protein–protein interactions between angiogenin and antiangiogenin antibody. Angiogenin (ANG) is a 14 kDa protein isolated from HT-29 human colon adenocarcinoma cells.<sup>32</sup> It is a potent blood vessel inducer implicated in both tumor growth and metastasis.<sup>33</sup>

## ■ EXPERIMENTAL SECTION

**Materials.** Phosphate-buffered saline (PBS, pH 7.4) was purchased from Amresco (Solon, OH). Bovine serum albumin (BSA) was purchased from USB Corporation (Santa Clara, CA). PD-10 desalting columns were purchased from GE Healthcare (Buckinghamshire, U.K.). Mineral oil and trichloro (1H,1H,2H,2H-perfluorooctyl) silane were both purchased from Sigma-Aldrich (St. Louis, MO) and used without further purification. ABIL EM 90 surfactant was obtained from Evonik Goldschmidt GmbH (Essen, Germany). FC-40 perfluorinated oil was purchased from Acros Organics (Geel, Belgium) and used without further purification. Polydimethylsiloxane (PDMS, Sylgard 184 silicone elastomer kit) was purchased from Dow Corning (Midland, MI). Alex Fluor 488 protein labeling kits were purchased from Invitrogen (Carlsbad, CA).

**Microfluidic Device Fabrication and Operation.** PDMS microfluidic devices were fabricated using standard soft lithographic techniques.<sup>34,35</sup> The PDMS prepolymer and curing agent were mixed in a ratio of 10:1 w/w and poured onto a patterned Si-wafer master. After curing on a hot plate at 70 °C for 2 h, the semicured PDMS block was peeled off and inlet and outlet holes were punched using a 1.5 mm diameter micro-punch. After oxygen plasma treatment for 40 s, the structured PDMS layer and glass slide were bonded immediately and cured on a 70 °C hot plate for approximately 1 h. Since, the size of droplets formed at microchannel T-junctions is primarily determined by the channel structure and the hydrophobicity of the channel surface,<sup>36</sup> PDMS devices were incubated in an oven at 70 °C for 4 h and treated with a solution of 2% trichloro (1H,1H,2H,2H-perfluorooctyl) silane in FC-40 to create uniformly hydrophobic PDMS channels.<sup>37,38</sup> Three input aqueous phases were used in all experiments and consisted of angiogenin labeled with Alexa Fluor 488 (AF488-ANG), anti-angiogenin antibody (anti-ANG Ab), and 0.1 mg/mL BSA in PBS. ABIL EM 90 (4%) in mineral oil was used as a carrier fluid. The microfluidic device was operated at volumetric flow rates ranging from 0.1 to 1.5  $\mu$ L/min using four precision syringe pumps (PHD2000, Harvard Apparatus). TYGON flexible plastic tubes (Buckeye Container Co.) were used to connect the microfluidic device with 1 mL NORM-JECT plastic syringes (Henke Sass Wolf, Germany).

**Preparation of Protein Samples.** Rosetta strain *Escherichia coli* (DE3)pLysS (carrying the plasmid pET-angiogenin) were used for the expression of angiogenin (ANG). Isolated inclusion bodies were dissolved in 7 M guanidine hydrochloride (GdnHCl), 20 mM Tris-HCl (pH 8.0), 10 mM EDTA, and 10 mM DTT and then incubated for 16 h at 4 °C. Refolding was achieved by dilution with 100 mM Tris-HCl (pH 8.0), 0.5 M L-Arg, 0.6 mM GSSG, and 3 mM GSH and then incubated for 24 h at 4 °C. Once folding was complete, the solution was concentrated by ultrafiltration and then loaded onto a cationic-exchange FPLC column packed with SP-Sepharose Fast Flow 4B stationary phase (GE Healthcare, U.K.) and equilibrated with 25 mM Tris-HCl (pH 8.0). Collected fractions from the FPLC column were dialyzed against PBS. Antiangiogenin

antibody (anti-ANG Ab) was isolated and purified as described previously.<sup>39</sup> The purified ANG was labeled with Alexa Fluor 488 (AF488), using the AF488 protein-labeling kit according to the manufacturer's protocol. The AF488-ANG was purified by using a PD-10 desalting column. Labeling efficiencies were assessed using the extinction coefficient for AF488 at 492 and 280 nm. The dye-to-protein ratio was calculated to be 0.53.

**Instrumentation.** The fluorescence spectrometer consisted of a 488 nm diode laser (10 mW, World Star Tech, Canada), an inverted fluorescence microscope (IX71, Olympus, Japan), and a dual polarization detection system. An electron multiplying-charge coupled device (ProEM EM-CCD, Princeton Instruments) was used for the detection of polarized emission in all experiments. The laser beam was introduced into the microscope body using beam-steering optic mirrors and then reflected by a dichroic mirror (FF506-Di02, Semrock) into an objective (20 $\times$ , Olympus, Japan). Fluorescence emission was collected using the same objective and spectrally filtered from the excitation using an emission filter (FITC-3540B, Semrock). Droplets were observed using a 20 $\times$  objective and EM-CCD operating at room temperature. All EM-CCD images were taken using the WinSpec/32 program (Princeton Instruments) using a 1 ms exposure time in binning mode.

**Bulk Fluorescence Polarization Measurements.** Time-integrated fluorescence polarization measurements were measured on the Beacon 2000 Fluorescence Polarization System (Invitrogen). For analysis of ANG and anti-ANG Ab interactions, 1.25 nM AF488-ANG was titrated with anti-ANG Ab (0.05–50 nM), and the fluorescence polarization was monitored. Values of  $K_D$  were determined by analyzing the data using GraphPad Prism 5.0 software.

## ■ RESULTS AND DISCUSSION

Interactions between ANG and anti-ANG Ab were investigated within 350 pL droplets using fluorescence polarization. Specifically, interaction between ANG and anti-ANG Ab was reported by labeling ANG with Alexa Fluor 488 (AF488-ANG) and monitoring variations in the polarization of emitted photons when anti-ANG Ab is added. It has previously been shown that ANG remains active after labeling with AF488.<sup>14</sup>

As shown in Figure 1a, when AF488-ANG is excited with 488 nm plane-polarized light, emission at 520 nm is largely depolarized since AF488-ANG (a small molecule) is able to rotate rapidly in solution during its fluorescence lifetime.<sup>40</sup> Conversely, if AF488-ANG is bound to anti-ANG Ab (a much larger macromolecule), its effective molecular volume is significantly increased and the rotation of AF488-ANG is hindered, resulting in less efficient depolarization. In basic terms, the bound and free states of AF488-ANG will have different polarization values: high for the bound state and low for the free state. Moreover, the measured polarization will be a weighted average of the two values, thus providing a direct measure of the fraction of AF488-ANG bound to anti-ANG Ab.

Droplet-based experiments were performed using a polydimethylsiloxane (PDMS) microfluidic device containing three aqueous inlets, one oil inlet and a single outlet. A schematic of the microfluidic device is shown in Figure 1b. Here, anti-ANG Ab is delivered through the left inlet, while AF488-ANG is delivered through the right inlet. A central buffer stream is introduced through the middle inlet to prevent mixing of the sample streams prior to droplet formation. Droplets have an average volume of approximately 350 pL and were generated at a frequency of 40 Hz.

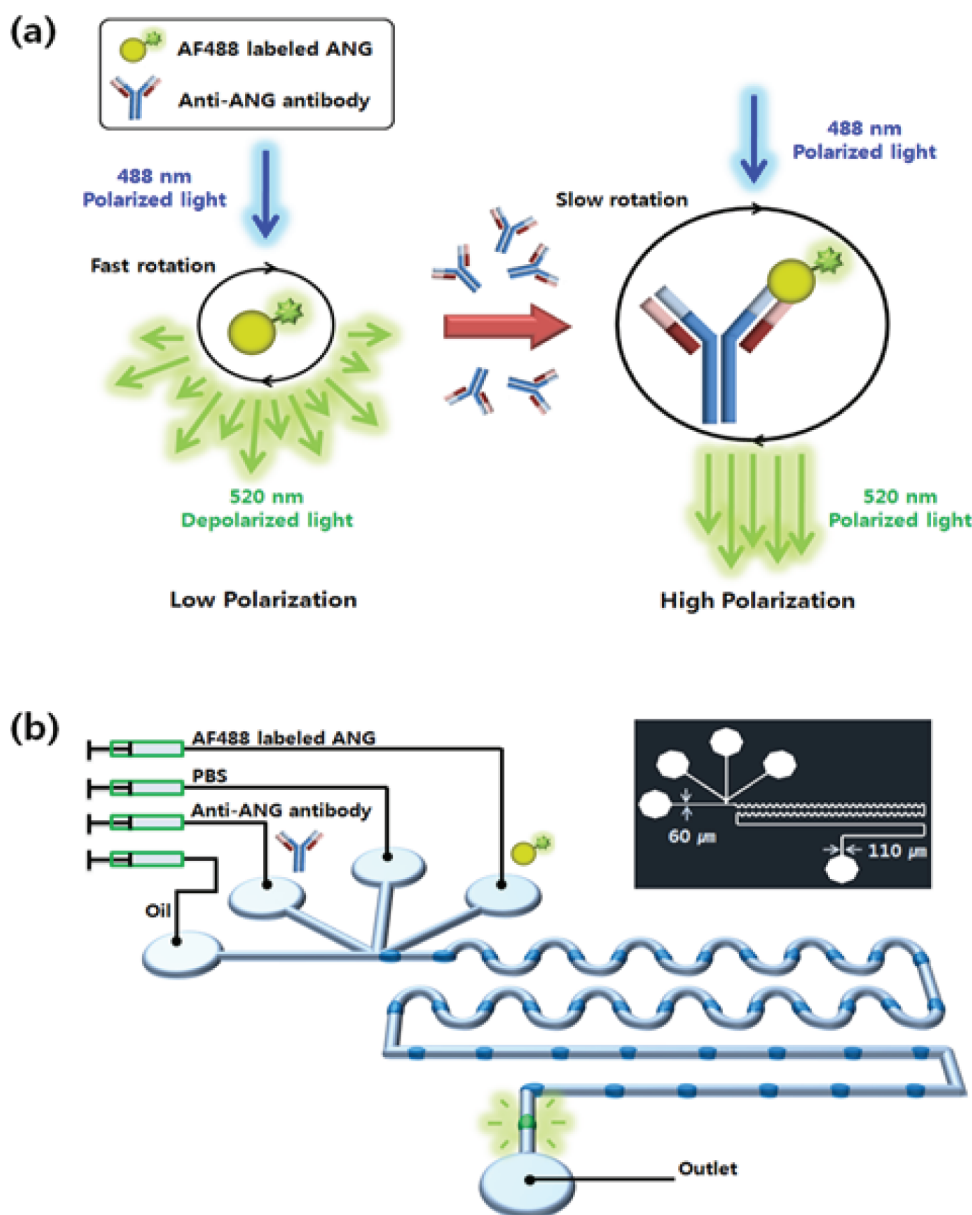


**Figure 1.** (a) Schematic of the concept behind fluorescence polarization analysis of protein–protein interactions. (b) Layout of the microfluidic device used for fluorescence polarization experiments. An AF488 labeled angiogenin (AF488-ANG) solution flowing from the right inlet, while antiangiogenin antibody (anti-ANG Ab) solution flows from the left inlet. The phosphate buffered saline (PBS, pH 7.4) is delivered into the middle inlet.

A schematic of the optical setup used for FP measurements is provided in Figure 2. Here, 488 nm radiation is passed through a vertical polarizer prior to excitation of fluorophores in the microfluidic channel. Only those molecules whose dipoles are oriented vertically will absorb radiation and subsequently emit light. Emitted radiation is concurrently measured in both vertical and horizontal planes using an EM-CCD detector.

To confirm the efficacy of our experimental approach, time-integrated fluorescence intensities and polarization were measured as a function of AF488-ANG concentration in multiple droplets. Specifically, the concentration of AF488-ANG was varied between 0 and 10 nM by changing the relative flow rates of AF488-ANG and PBS streams from 0.1 to 0.9  $\mu\text{L}/\text{min}$ , while the total aqueous flow rate was kept constant, maintaining both

droplet size and generation frequency. The water fraction ( $W_f$ ) can be expressed as

$$W_f = F_w / (F_w + F_o) \quad (1)$$

Here  $F_w$  and  $F_o$  define the aqueous flow rates and oil flow rates, respectively.<sup>41,42</sup>

Figure 3a,b reports the variation of time-integrated fluorescence as a function of ANG concentration in both bulk and droplet environments. Over the concentration range studied, this variation is linear and yields an analytical sensitivity of  $50.6 \times 10^6$  counts/M for droplet-based measurements and  $51.5 \times 10^6$  counts/M for bulk measurements. Figure 3c,d describes the variation of fluorescence polarization over an identical concentration range. Not surprisingly, in both environments the polarization is of low magnitude and demonstrates no significant variation with ANG concentration.



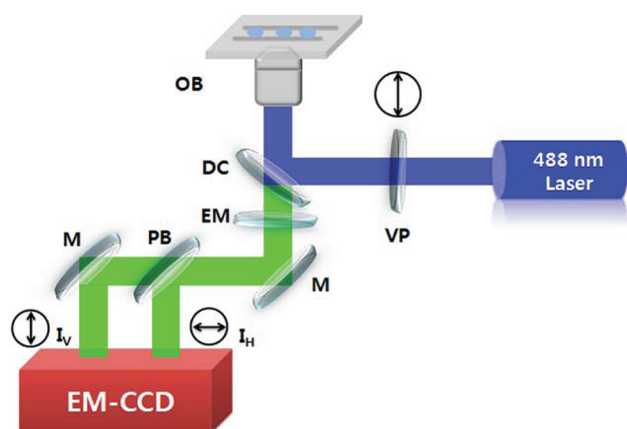


**Figure 2.** Schematic of the optical setup used for fluorescence polarization measurements. The system consists of a 20× OB, DC, EM, VP, M, PB, 488 nm laser, and EM-CCD (OB, objective; DC, dichroic mirror; EM, emission filter; VP, vertical polarizer; M, mirror; PB, polarizing beam splitter; EM-CCD, electron multiplying-charge coupled device).  $I_v$  and  $I_h$  define the vertical intensity of the emission light and the horizontal intensity of the emission light, respectively. A dual fluorescence polarization detection system was used to simultaneously record  $I_v$  and  $I_h$  from the AF488 labeled angiogenin (AF488-ANG) in the presence or absence of antiangiogenin antibody (anti-ANG Ab).

Finally, the interaction between ANG and anti-ANG Ab was analyzed using fluorescence polarization within microdroplets. Solutions of AF488-ANG, BSA in PBS (0.1 mg/mL), and anti-ANG Ab were injected through the right inlet, middle inlet, and left inlet, respectively. The BSA in PBS solution (at pH 7.4)

was used to both inhibit nonspecific interaction of reagents with channel walls (in the inlet region) and separate AF488-ANG and anti-ANG Ab streams prior to droplet formation. Accordingly, online dilution was performed by varying the relative flow rates of anti-ANG Ab and PBS streams from 0.1 to 0.9  $\mu\text{L}/\text{min}$ , but keeping the AF488-ANG flow rate at 0.5  $\mu\text{L}/\text{min}$ . The total aqueous flow rate was kept constant to maintain both the droplet size and generation frequency. Using these conditions, AF488-ANG was maintained at a concentration of 5 nM, while anti-ANG Ab was varied between 0.4 and 54 nM.

Typical  $I_v$  and  $I_h$  fluorescence burst scans over a time period of 500 ms are presented in Figure 4. It is observed that both  $I_v$  and  $I_h$  decrease as a function of anti-ANG Ab concentration. Polarization values are then calculated from  $I_v$  and  $I_h$  using the following formula

$$P = (I_v - I_h) / (I_v + I_h) \quad (2)$$

Figure 5 illustrates the variation in polarization as a function of anti-ANG Ab concentration. It can be seen that polarization increases with anti-ANG Ab concentration asymptotically approaching a maximum value at high anti-ANG Ab concentrations. The variation in polarization due to the interaction between AF488-ANG and anti-ANG Ab were modeled using the following function,<sup>14</sup>

$$P = P_{\min} + \Delta P \left( \frac{[\text{anti-ANGAb}]}{K_D + [\text{anti-ANGAb}]} \right) \quad (3)$$

where  $P$ ,  $\Delta P$ , and  $[\text{anti-ANG Ab}]$  are the measured polarization, total change in polarization, and the total concentration of

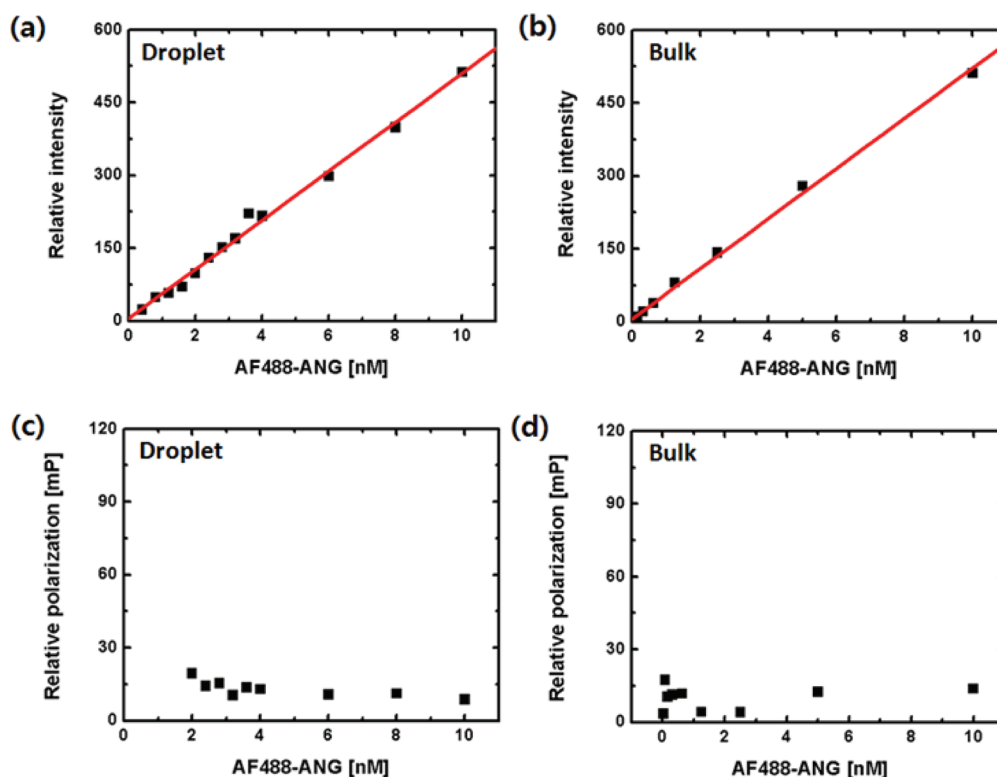


**Figure 3.** Fluorescence intensity (a, b) and polarization (c, d) versus the concentration of the angiogenin labeled with AF488 (AF488-ANG) in (a, c) a droplet-based microfluidic system and in (b, d) a bulk fluorescence/polarization setup. In the droplet-based microfluidic system, the concentration of AF488-ANG was varied (0–10 nM) by changing the relative flow rates of AF488-ANG and PBS streams from 0.1 to 0.9  $\mu\text{L}/\text{min}$  while the total aqueous flow rate was kept constant to maintain droplet size and generation frequency.

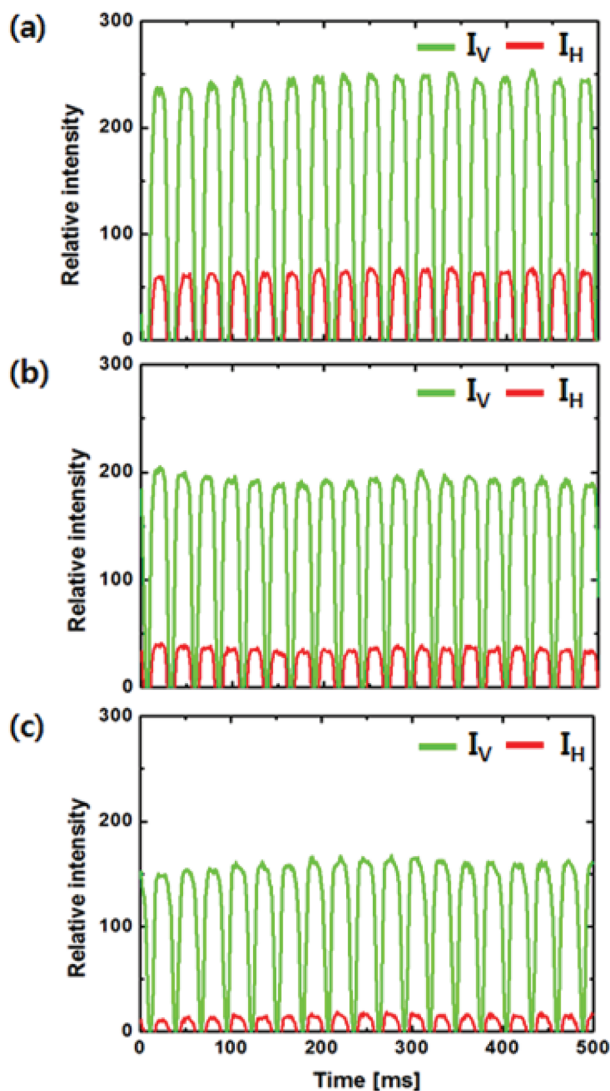


**Figure 4.** Exemplar fluorescence burst scans recorded over a time period of 500 ms. The concentration of the angiogenin labeled with Alexa Fluor 488 (AF488-ANG) was fixed at 5 nM, while the concentration of anti-angiogenin antibody (anti-ANG Ab) was varied between (a) 0.8 nM, (b) 12 nM, and (c) 45 nM. Green lines represent  $I_V$ , and red lines represent  $I_H$ .

anti-ANG Ab, respectively. A nonlinear least-squares fit to the data yields  $K_D = 10.4 \pm 3.3$  nM,  $P_{\min} = 7.6 \pm 5.8$  mP, and  $\Delta P = 108.1 \pm 6.2$  mP (Figure 5a). For a comparison,  $K_D = 4.1 \pm 0.9$  nM extracted from bulk experiments (Figure 5b) and  $K_D = 16.6 \pm 2.4$  nM from previous droplet-based experiments using time-integrated fluorescence detection.<sup>14</sup> The error in the  $K_D$  value of this method is higher than that of other methods. The error in this value can be reduced simply by increasing the number of droplets interrogated.

## CONCLUSIONS

Herein, we have demonstrated for the first time the use of fluorescence polarization and droplet-based microfluidics for the rapid analysis of protein–protein interactions. Specifically, the interaction between angiogenin (ANG) and antiangiogenin antibody (anti-ANG Ab) was successfully analyzed in short times and with high precision. The time scale is calculated through knowledge of the droplet volume and droplet generation frequency. The precision of the extracted data is directly related to the number of experiments performed. In the current experiments,  $K_D$  is extracted from the analysis of about 10 000 droplets. The error in this value can be reduced simply by increasing the number of droplets interrogated while still ensuring much shorter analysis time than for bulk assays.

When operating at a droplet generation frequency of 40 Hz and an average droplet volume of 350 pL, only 14 nL of sample is required per experiment. This represents a reduction of 4 orders of magnitude when compared to equivalent bulk assays. In this study, the samples are loaded from a syringe pump with an associated dead volume, but each droplet can be preformed and stored in the external device such as capillary tubing by using in-house robotic samplers. This means that the entirety of the sample volume can be analyzed.

A significant advantage when using fluorescence polarization to report protein–protein interactions is the requirement for only one labeled molecule. As noted, this contrasts with other approaches such as FRET, which necessitate the labeling of both ligand and analyte. Importantly this means that the droplet-based fluorescence polarization assay format described is suitable for diagnostic measurements where the concentration of a disease-related protein, DNA, or RNA can be assessed without

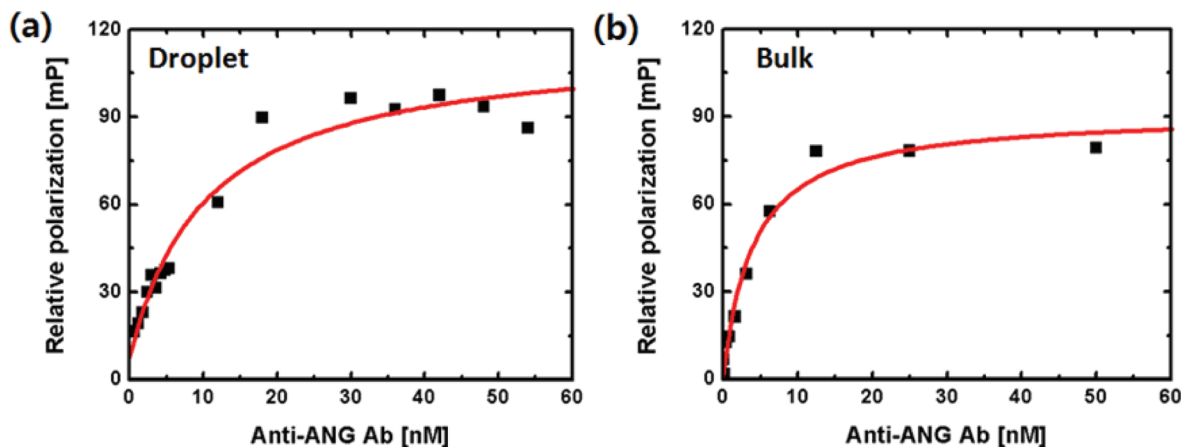


**Figure 5.** Analysis of binding of angiogenin (ANG) with antiangiogenin antibody (anti-ANG Ab) by fluorescence polarization. (a) In the droplet-based microfluidic system, the concentration of the angiogenin labeled with Alexa Fluor 488 (AF488-ANG) was fixed at 5 nM, while the concentration of anti-ANG Ab varied between 0 and 54 nM. (b) In bulk experiments, the concentration of AF488-ANG was fixed at 1.25 nM, while the concentration of anti-ANG Ab was varied between 0 and 50 nM.

the need for sample purification or separation. We are currently exploring applications toward this goal.

## AUTHOR INFORMATION

### Corresponding Author

\*E-mail: sichang@chungbuk.ac.kr.

### Notes

The authors declare no competing financial interest.

## ACKNOWLEDGMENTS

This work was supported by the Global Research Laboratory Program of the National Research Foundation of Korea (NRF) funded by the Ministry of Education, Science, and Technology (MEST) of Korea (Grant Number K20904000004-11A0500-00410). We are grateful to Mr. Soongwon Cho at Imperial College London for contributive discussions and Prof. Dong-Hun Lee at Chungbuk National University for the droplet analysis program.

## REFERENCES

- (1) Huebner, A.; Sharma, S.; Srisa-Art, M.; Hollfelder, F.; Edel, J. B.; deMello, A. J. *Lab Chip* **2008**, *8*, 1244–1254.
- (2) Cho, S.; Kang, D. K.; Choo, J.; deMello, A. J.; Chang, S. I. *BMB Rep.* **2011**, *44*, 705–712.
- (3) Whitesides, G. M. *Nature* **2006**, *442*, 368–373.
- (4) Song, H.; Chen, D. L.; Ismagilov, R. F. *Angew. Chem., Int. Ed.* **2006**, *45*, 7336–7356.
- (5) Theberge, A. B.; Courtois, F.; Schaerli, Y.; Fischlechner, M.; Abell, C.; Hollfelder, F.; Huck, W. T. *Angew. Chem., Int. Ed.* **2010**, *49*, 5846–5868.
- (6) Song, H.; Bringer, M. R.; Tice, J. D.; Gerds, C. J.; Ismagilov, R. F. *Appl. Phys. Lett.* **2003**, *83*, 4664–4666.
- (7) Song, H.; Ismagilov, R. F. *J. Am. Chem. Soc.* **2003**, *125*, 14613–14619.
- (8) Srisa-Art, M.; deMello, A. J.; Edel, J. B. *Phys. Rev. Lett.* **2008**, *101*, 014502.
- (9) Casadevall, i. Solvas, X.; Srisa-Art, M.; deMello, A. J.; Edel, J. B. *Anal. Chem.* **2010**, *82*, 3950–3956.
- (10) Niu, X.; Gielen, F.; Edel, J. B.; deMello, A. J. *Nat. Chem.* **2011**, *3*, 437–442.
- (11) Wei, Q.; Lee, M.; Yu, X.; Lee, E. K.; Seong, G. H.; Choo, J.; Cho, Y. W. *Anal. Biochem.* **2006**, *358*, 31–37.
- (12) Srisa-Art, M.; deMello, A. J.; Edel, J. B. *Anal. Chem.* **2007**, *79*, 6682–6689.
- (13) Jung, J.; Chen, L.; Lee, S.; Kim, S.; Seong, G. H.; Choo, J.; Lee, E. K.; Oh, C. H.; Lee, S. *Anal. Bioanal. Chem.* **2007**, *387*, 2609–2615.
- (14) Srisa-Art, M.; Kang, D. K.; Hong, J.; Park, H.; Leatherbarrow, R. J.; Edel, J. B.; Chang, S. I.; deMello, A. J. *ChemBioChem* **2009**, *10*, 1605–1611.
- (15) Chan, K. L.; Niu, X.; deMello, A. J.; Kazarian, S. G. *Anal. Chem.* **2011**, *83*, 3606–3609.
- (16) Tian, R.; Hoa, X. D.; Lambert, J. P.; Pezacki, J. P.; Veres, T.; Figeys, D. *Anal. Chem.* **2011**, *83*, 4095–4102.
- (17) Chon, H.; Lim, C.; Ha, S. M.; Ahn, Y.; Lee, E. K.; Chang, S. I.; Seong, G. H.; Choo, J. *Anal. Chem.* **2010**, *82*, 5290–5295.
- (18) Cecchini, M. P.; Hong, J.; Lim, C.; Choo, J.; Albrecht, T.; deMello, A. J.; Edel, J. B. *Anal. Chem.* **2011**, *83*, 3076–3081.
- (19) Checovich, W. J.; Bolger, R. E.; Burke, T. *Nature* **1995**, *375*, 254–256.
- (20) Bolger, R.; Wiese, T. E.; Ervin, K.; Nestich, S.; Checovich, W. *Environ. Health Perspect.* **1998**, *106*, 551–557.
- (21) Murakami, A.; Nakaura, M.; Nakatsuji, Y.; Nagahara, S.; Tran-Cong, Q.; Makino, K. *Nucleic Acids Res.* **1991**, *19*, 4097–4102.
- (22) Lundblad, J. R.; Laurance, M.; Goodman, R. H. *Mol. Endocrinol.* **1996**, *10*, 607–612.
- (23) Ozers, M. S.; Hill, J. J.; Ervin, K.; Wood, J. R.; Nardulli, A. M.; Royer, C. A.; Gorski, J. *J. Biol. Chem.* **1997**, *272*, 30405–30411.
- (24) Wu, P.; Brasseur, M.; Schindler, U. *Anal. Biochem.* **1997**, *249*, 29–36.
- (25) Jiskoot, W.; Hoogerhout, P.; Beuvery, E. C.; Herron, J. N.; Crommelin, D. J. *Anal. Biochem.* **1991**, *196*, 421–426.
- (26) Wei, A. P.; Herron, J. N. *Anal. Chem.* **1993**, *65*, 3372–3377.
- (27) Bolger, R.; Checovich, W. *Biotechniques* **1994**, *17*, 585–589.
- (28) Bolger, R.; Thompson, D. *Am. Biotechnol. Lab.* **1994**, *12*, 113–116.
- (29) Levine, L. M.; Michener, M. L.; Toth, M. V.; Holwerda, B. C. *Anal. Biochem.* **1997**, *247*, 83–88.
- (30) Wang, H.; Lu, M.; Tang, M. S.; Van Houten, B.; Ross, J. B.; Weinfeld, M.; Le, X. C. *Proc. Natl. Acad. Sci. U.S.A.* **2009**, *106*, 12849–12854.
- (31) Zahng, D.; Lu, M.; Wang, H. *J. Am. Chem. Soc.* **2011**, *133*, 9188–9191.
- (32) Fett, J. W.; Strydom, D. J.; Lobb, R. R.; Alderman, E. M.; Bethune, J. L.; Riordan, J. F.; Vallee, B. L. *Biochemistry* **1985**, *24*, 5480–5486.
- (33) Yoshioka, N.; Wang, L.; Kishimoto, K.; Tsuji, T.; Hu, G. F. *Proc. Natl. Acad. Sci. U.S.A.* **2006**, *103*, 14519–14524.
- (34) Beard, N. P.; Edel, J. B.; deMello, A. J. *Electrophoresis* **2004**, *25*, 2363–2373.
- (35) Gao, R.; Choi, N.; Chang, S. I.; Kang, S. H.; Song, J. M.; Cho, S. I.; Lim, D. W.; Choo, J. *Anal. Chim. Acta* **2010**, *681*, 87–91.
- (36) Li, L.; Mustafa, D.; Fu, Q.; Tereshko, V.; Chen, D. L.; Tice, J. D.; Ismagilov, R. F. *Proc. Natl. Acad. Sci. U.S.A.* **2006**, *103*, 19243–19248.
- (37) Roach, L. S.; Song, H.; Ismagilov, R. F. *Anal. Chem.* **2005**, *77*, 785–796.
- (38) Wang, D.; Goel, V.; Oleschuk, R. D.; Horton, J. H. *Langmuir* **2008**, *24*, 1080–1086.
- (39) Chang, S. I.; Jeong, G. B.; Park, S. H.; Ahn, B. C.; Choi, J. D.; Namgong, S. K.; Chung, S. I. *Biochem. Biophys. Res. Commun.* **1997**, *232*, 323–327.
- (40) Perrin, F. *J. Phys. Radium* **1926**, *7*, 390–401.
- (41) Garstecki, P.; Fuerstman, M. J.; Stone, H. A.; Whitesides, G. M. *Lab Chip* **2006**, *6*, 437–446.
- (42) Song, H.; Li, H. W.; Munson, M. S.; Van Ha, T. G.; Ismagilov, R. F. *Anal. Chem.* **2006**, *78*, 4839–4849.